



# EUROfusion

EUROFUSION WPMST1-PR(16) 15027

J Schweinzer et al.

## **Development of the Q=10 Scenario for ITER on ASDEX Upgrade (AUG)**

Preprint of Paper to be submitted for publication in  
Nuclear Fusion



This work has been carried out within the framework of the EUROfusion Consortium and has received funding from the Euratom research and training programme 2014-2018 under grant agreement No 633053. The views and opinions expressed herein do not necessarily reflect those of the European Commission.

This document is intended for publication in the open literature. It is made available on the clear understanding that it may not be further circulated and extracts or references may not be published prior to publication of the original when applicable, or without the consent of the Publications Officer, EUROfusion Programme Management Unit, Culham Science Centre, Abingdon, Oxon, OX14 3DB, UK or e-mail [Publications.Officer@euro-fusion.org](mailto:Publications.Officer@euro-fusion.org)

Enquiries about Copyright and reproduction should be addressed to the Publications Officer, EUROfusion Programme Management Unit, Culham Science Centre, Abingdon, Oxon, OX14 3DB, UK or e-mail [Publications.Officer@euro-fusion.org](mailto:Publications.Officer@euro-fusion.org)

The contents of this preprint and all other EUROfusion Preprints, Reports and Conference Papers are available to view online free at <http://www.euro-fusionscipub.org>. This site has full search facilities and e-mail alert options. In the JET specific papers the diagrams contained within the PDFs on this site are hyperlinked

## Development of the Q=10 Scenario for ITER on ASDEX Upgrade (AUG)

J. Schweinzer 1), M. Beurskens 1), L. Frassinetti 2), E. Joffrin 3), V. Bobkov 1), R. Dux 1), R. Fischer 1), C. Fuchs 1), A. Kallenbach 1), C. Hopf 1), P.T. Lang 1), A. Mlynek 1), T. Pütterich 1), F. Ryter 1), J. Stober 1), G. Tardini 1), E. Wolfrum 1), H. Zohm 1) the EUROfusion MST1 Team \*) and the ASDEX Upgrade Team

1) Max Planck Institute for Plasma Physics, 85748 Garching, Germany

2) KTH, Division of Fusion Plasma Physics, SE-10044 Stockholm, Sweden

3) CEA, Centre de Cadarache, 13108 Saint Paul-lez-Durance, France

\*) See <http://www.euro-fusionscipub.org/mst1>.

E-mail contact of main author: [josef.schweinzer@ipp.mpg.de](mailto:josef.schweinzer@ipp.mpg.de)

**Abstract.** The development of the baseline H-mode scenario foreseen for ITER on the ASDEX Upgrade tokamak, i.e. discharges at  $q_{95}=3$ , relatively low  $\beta_N \sim 1.8$ , high normalized density  $n/n_{GW} \sim 0.85$  and high triangularity  $\delta=0.4$ , focused on the integration of elements foreseen for ITER and available on ASDEX Upgrade, such as ELM mitigation techniques and impurity seeding in combination with a metallic wall. Values for density and energy confinement simultaneously came close to the requirements of the ITER baseline scenario as long as  $\beta_N$  stayed above 2. At lower heating power and thus lower  $\beta_N$  normalized energy confinement  $H_{98y2} \sim 0.85$  is obtained. It has been found that stationary discharges are not easily achieved under these conditions due to the low natural ELM frequency occurring at the low  $q_{95}$  / high  $\delta$  operational point. Up until now the ELM parameters were uncontrollable with the tools developed in other scenarios. Therefore studies on an alternative operational point at higher  $\beta_N$  and  $q_{95}$  have been conducted. In order to prepare for the ITER first non-activation operational phase, Helium operation has been investigated as well.

### 1. Introduction

In ITER, H-mode operation at 15MA and  $q_{95}=3$  is planned to achieve 500MW fusion power at Q=10 in deuterium-tritium mixtures. This so-called ITER baseline (BL) scenario is

characterized by normalized parameters for plasma density  $f_{\text{GW}}=n/n_{\text{GW}}=0.85$ , energy confinement  $H_{98y2}\sim 1$  and beta  $\beta_N\sim 1.8$  [1]. Based on results from tokamaks with a carbon wall, a high triangularity shape ( $\delta=\delta_{\text{average}}\sim 0.4$ ) has been identified to be best suited in ITER to combine high density operation using permanent deuterium gas dosing with good H-mode confinement [2 and references therein]. The metallic wall of AUG requires central wave-heating (ECRH or ICRF) to avoid core tungsten impurity accumulation. This boundary condition of needing RF power centrally deposited in the plasma, limits the possible values for plasma current  $I_p$  and magnetic field  $B_t$  to a few practical combinations of  $I_p / B_t$ . In particular, two routes [3] have been explored for  $q_{95}=3$  plasmas on AUG: (i) operation at 1.1MA/1.8T using ECRH at 140GHz in X3 mode and (ii) 1.2MA/2T using ICRH at 30MHz from two antennas with boron-coated protection limiter tiles.

This paper will discuss the present status of ITER BL demonstration plasmas on AUG based on experiments carried out between 2012 and 2014 and will describe attempts to mitigate ELMs in this scenario as well as on a slight shift of the scenario's operational point towards a potential 'less difficult corner' at 20% lower  $I_p$  (higher  $q_{95}$ ).

## 2. Behaviour of $q_{95}=3$ ITER BL discharges on AUG

A typical example for the demonstration of the ITER BL scenario at 1.2MA / 2T can be seen in fig. 1. Such discharges are typically ramped up to 1MA in a low- $\delta$  shape, followed by a combined slow ramp of  $I_p$  and  $\delta$  until the flattop is reached and sustained for several seconds. A feed-forward gas fuelling rate is slowly raised up to a flattop value of typically  $\sim 2.5\cdot 10^{22}$  atoms/s. Such a puff rate corresponds to a divertor neutral pressure of about 1.7 Pa. In several discharges stationary behaviour is obtained in the flattop and parameters  $H_{98y2}$  and  $f_{\text{GW}}$  simultaneously come close to the target values of 1 and 0.85, respectively [3, 4]. Although the amount of applied heating power in the standard heating recipe for such discharges is already at the lower end for AUG,  $\beta_N$  typically stays at values 20% above the ITER target of 1.8. Thus, for a full demonstration of an ITER BL plasma on AUG, normally too much additional heating power is applied, which is on the other hand helpful for an effective impurity flushing by ELMs.

During the ramp-up of  $I_p$  and  $\delta$ , the ELM signature of such ITER BL discharges changes. While in the early phase (low  $\delta$ ,  $q_{95}\sim 3.5$ ) the ELM frequency  $f_{\text{ELM}}$  is high at 100 Hz, and the energy loss per ELM  $\Delta W_{\text{ELM}}$  at 20-40 kJ is low, the situation reverses once both parameters  $\delta$  and  $q_{95}$  approach their flattop values of 0.36 and 3 respectively. In the fully shaped flattop low

ELM-frequencies of 10 - 25 Hz are typical as well as large energy losses  $\Delta W_{\text{ELM}}$  values of 40 – 120 kJ, which means 5% – 15% losses of stored energy per ELM event which are intolerable in view of ITER [5].

The operational window for the ITER BL scenario on AUG where a stationary behaviour is possible and W accumulation can be avoided is set by the following (inter-linked) parameters:

- Closeness to the last boronization / quality of wall conditioning;
- Deuterium gas puff level;
- Heating power in total and in particular the amount centrally deposited;

With well conditioned walls, i.e. a few days after a boronization, the gas puff level could be reduced to  $1.5 \cdot 10^{22} \text{ s}^{-1}$  being then close to the onset of W accumulation. Many stationary discharges were conducted for D puff levels between  $2 \cdot 10^{22} \text{ s}^{-1}$  and  $3 \cdot 10^{22} \text{ s}^{-1}$ . Only in such phases with well conditioned walls could ITER BL ( $I_p = 1.1$  or  $1.2$  MA) discharges with  $P_{\text{NBI}} < 5\text{MW}$  be sustained, or the central RF heating could be reduced to low values of less than 1MW.

For ITER BL attempts where the beneficial effect of boronization was lacking, stable discharges could only be produced at gas puff levels  $\geq 3.8 \cdot 10^{22}$  and at a total heating power exceeding 6.8 MW. Only within this reduced operational window could  $f_{\text{ELM}}$  be kept sufficiently high to allow an effective flushing of impurities necessary to avoid W accumulation. The two BL discharges (#28361 and #29958) in fig. 2 mainly differ in the number of discharges performed since the last boronization. Although the gas puff is twice as high in #29958 (21 days after boronization),  $f_{\text{ELM}}$  is just half of the value observed in #28361 (1 day after boronization). The gas puff rate of  $3.8 \cdot 10^{22} \text{ 1/s}$  turned out to be the lower limit for the machine / wall condition of #29958, because it lead to ELMs ( $f_{\text{ELM}} = 12 \text{ Hz}$ ) which are just frequent enough for an effective removal of impurities (in particular W) out of the pedestal. Thus, under such conditions only H-factors between 0.8 and 0.85 are possible. Attempts with a lower gas puff rate to improve the confinement produced even lower  $f_{\text{ELM}}$  and were terminated by W accumulation.

In ASDEX Upgrade, where nitrogen seeding is a common recipe for power load reduction, the first wall gets loaded with N. As a result, the intensity of a nitrogen N II emission line (399.5 nm) on an outboard limiter (4<sup>th</sup> box in fig. 2) - being a measure for the influx of an expected broad spectrum of medium-Z impurities from the wall - is a good indicator for the wall condition. Right after a boronization (#28361, in fig. 2), the residential N is covered up and the level of this line is one order of magnitude smaller than in the case (#29958) where

the effect of boronization is lacking. Thus, the considerably different composition of the edge plasma with respect to low-Z impurities released by the first wall also has a significant impact on the tungsten concentration ( $c_w$ , see fig. 2) which is almost an order of magnitude larger in the case (#29958) where the effect of boronization is lacking. With the higher tungsten concentration - on AUG tungsten is mainly sputtered by medium-Z impurities from the main chamber wall - also the core radiation level increases (see fig. 2) which leads to a decreasing ELM-frequency ( $f_{\text{ELM}}$ ), because less power is crossing the separatrix. The ITER BL scenario on AUG is in particular sensitive to the quality of wall conditioning / closeness to boronization because the ELM-frequency already under good conditions is low and a further reduction by the described mechanism leads to insufficient impurity flushing of the pedestal by ELMs and finally to situation where central impurity accumulation cannot be avoided.

### 3. Possible optimization of the ‘operational point’

Since the operation at  $q_{95} = 3$  and  $\beta_N < 2$  turned out to be difficult in particular with respect to stationarity and the ELM behaviour, H-modes at the same toroidal field, but at lower  $I_p$  (higher  $q_{95}$ ) were explored which still fulfil the requirement of  $Q=10$ . Keeping the fusion power  $P_{\text{fus}} \sim (\beta_N / q_{95})^2$  and the fusion gain factor  $G = Q / (Q+5) = 10.8 H_{98y2}^3 / (\beta_N \cdot q_{95}^2)$  [6] constant at the values of the ITER BL scenario, alternative values for  $H_{98y2}$  and  $\beta_N$  can be derived for a chosen  $q_{95}$ . Following this approach, target values for  $\beta_N = 2.2$  and  $H_{98y2} = 1.2$  are required for a chosen safety factor  $q_{95}$  of 3.6. As expected, lower values of  $I_p$  have to be compensated by higher H-factors. At even higher  $q_{95}$  the requirements for  $H_{98y2}$  and for  $f_{\text{GW}}$  become unrealistically high, hence  $q_{95} = 3.6$  is selected. A further assumption of keeping the same absolute (pedestal top) density as for the current BL  $q_{95}=3$  reference case, implies higher Greenwald fractions  $f_{\text{GW}}$  for the new alternative scenarios (at higher  $q_{95}$ ). On AUG we have therefore explored the operational behaviour of plasmas at 2.0T / 1.0 MA with a safety factor  $q_{95} = 3.6$  in the ITER BL shape with target values of  $\beta_N = 2.2$ ,  $H_{98y2} = 1.2$  and  $0.8 \leq f_{\text{GW}} \leq 0.95$ . For ITER this would mean operation at 5.3T / 12.5 MA instead of 5.3T / 15MA. This new alternative scenario and its comparison with the reference case, will give better insight into whether working at lower  $I_p$  is actually an advantage or leads to other operational problems due to the increased requirements for normalized confinement  $H_{98y2}$  and density  $f_{\text{GW}}$ .

#### 4. Behaviour of the $q_{95}=3.6$ 'alternative ITER BL' discharges

In the following (see fig. 3) we compare an 'alternative' ITER BL discharge at 1.0 MA with a safety factor  $q_{95} = 3.6$  to an ITER BL  $q_{95}=3$  discharge at 1.2 MA. Both discharges are at the same toroidal field  $B_t = 2T$ . The applied heating power (NBI + ICRH) is kept the same, and the plasma shape is very similar. The NBI power at 3.6 MW (by reducing the beam voltage of one NBI box to 60 kV) has been chosen to achieve a normalized pressure  $\beta_N$  close to the target value of 1.8 for the  $q_{95}=3$  case (#31146). With this reduced heating power (the previously used minimum NBI power for ITER BL demonstration plasmas at AUG is 5 MW) impurity accumulation could only be avoided by using a high  $D_2$  gas puff rate of  $3.1 \cdot 10^{22} \text{ s}^{-1}$ . This gas puff level turned out to be sufficient to counteract the anticipated smaller ELM frequency caused by the reduction of the NBI heating power and has to be considered to be at the lower end to achieve stationary conditions.

For a comparison discharge at the lower  $I_p = 1MA$  / higher  $q_{95} = 3.6$  (#31148) the only parameter to choose was the gas puff rate. It turned out that at  $q_{95} = 3.6$  this parameter ( $1.5 \cdot 10^{22} \text{ s}^{-1}$ ) could be considerably smaller than in the  $q_{95}=3$  case without losing stationarity of the plasma. Although plasma currents are different, the stored energy  $W_{MHD}$  in both discharges is the same (see fig. 3, upper, right box). The confinement factor  $H_{98y2}$  is 0.91 (at  $\beta_N=1.87$ ) for  $q_{95}=3$  and 1.05 (at  $\beta_N=2.15$ ) for  $q_{95}=3.6$ . This increase in H-factor of 15% is promising, but the absolute value of 1.05 is below the target of 1.2. The absorbed heating power  $P_{net}$  is 30 - 40% above the H-mode power threshold. The normalized pressure  $\beta_N$  is higher by 20% in the  $q_{95}=3.6$  case. It was not possible to keep the plasma density fixed, but the Greenwald densities  $f_{GW}$  of both discharges are almost identical and above the ITER target of 0.85 once the full shaping is reached after 3.2s. In the  $q_{95}=3.6$  discharge (#31148) between 4.8s and 6s a magnetic perturbation (MP)  $n=2$  field was switched on (indicated in both upper boxes of fig. 3) in order to test its influence on ELMs. Unfortunately the application of MP leads only to a degradation of both energy and particle confinement, but has no effect on ELMs.

In fig. 4 radial profiles of electron density and electron pressure averaged from 3.5s to 4.5s are shown for both discharges of fig. 3 (same colour code applies). Density profiles are almost flat. Central  $n_e$  values scale with the plasma current leading to identical  $f_{GW}$ . Electron temperatures are higher at the lower current leading to higher central electron pressure.

Scaling the plasma current down has provided a promising scenario at increased  $q_{95} \sim 3.6$ . Optimisation criteria are increasing central density by a further 15% and increasing  $H_{98y2}$  from 1.05 to 1.2. The main tools AUG has available to achieve this is an optimisation of particle fuelling by gas puff and pellets and the introduction of nitrogen for confinement improvement.

## 5. ELM mitigation attempts including Nitrogen seeding

In fig. 5 the normalized ELM energy loss ( $\Delta W_{\text{ELM}} / W_{\text{ped}}$ ) is plotted versus the pedestal plasma collisionality. ELM energy loss values for both BL scenarios at  $q_{95} = 3$  and  $q_{95} = 3.6$  are compared with those of a multi-machine database compiled by Loarte [5] and exceed the general trend considerably. The observed large ELMs are intolerable and their mitigation / suppression is mandatory in view of ITER.

Therefore, three methods [3] for ELM mitigation were first tried in the  $q_{95}=3$  ITER BL scenario: (i) ELM pace making with pellets ( $v_p = 560$  m/s) of different mass ( $m_p = 1.5 - 2.4 \cdot 10^{20}$  D atoms) and frequency (20-70 Hz) injected from the HFS, (ii) application of MP coils and (iii) nitrogen seeding.

In the all-W AUG pellet injection for pace making ceased to be a reliable ELM trigger [7] in purely  $D_2$  fuelled plasmas. Therefore in such plasmas  $f_{\text{ELM}}$  never reached the pellet repetition frequency. However, recently it was found that the presence of N can recover the pellet ELM trigger potential [7]. In an N-seeded  $q_{95}=3$  discharge - although at low  $\delta$  and with more  $P_{\text{NBI}}$  (7.5 MW) than typical for an ITER BL ( $P_{\text{NBI}} \leq 5$  MW) plasma - pellets launched at rates ramped from 20 up to 47 Hz triggered ELMs reliably. A first attempt to promote such improved triggering of ELMs by combining N seeding with pellet pacing at 70 Hz (#31151,  $t > 4.0$  s) to the  $q_{95}=3$  ITER BL scenario was conducted. In a phase 300ms before the first pellet was launched, N was introduced which reduced  $f_{\text{ELM}}$  from 17 to 10 Hz. In the 'pellet + N'-phase the  $D_2$  puff rate was reduced by a factor of two to keep the total fuelling by  $D_2$  puff and pellets similar to the previous phase with  $D_2$  puffing only. In this 'pellet + N' phase some pellets triggered ELMs, others still failed to do so, leading transiently to a  $f_{\text{ELM}}$  of 50 Hz. Surprisingly, this boost of  $f_{\text{ELM}}$  did not prevent impurity accumulation and density peaking. It seems that the optimal combination of puff rates for  $D_2$ , N and the pellet parameters (mass, repetition rate) has not been found yet.

AUG's ELM suppression scenario with magnetic perturbation (MP) fields, which works above a certain density or collisionality threshold [8], should in principle be compatible with



the ITER BL scenario. The application of MP coils in the ITER BL scenario slightly influenced both density and stored energy, but did not mitigate or even suppress ELMs. Although the required edge density for ELM suppression - found in another discharge with the same plasma shape (#29842), but at much higher  $q_{95}=5.5$  - was reached, no mitigation of ELMs was observed. The reason for this might be the lower collisionality due to the lower  $q_{95}$  in the ITER BL case.

Seeding of N normally increases  $f_{\text{ELM}}$  and reduces the ELM size in AUG plasmas whereas in the few  $q_{95}=3$  ITER BL attempts with N seeding  $f_{\text{ELM}}$  was in fact reduced. These discharges showed a slightly improved confinement, but were even more prone to W accumulation than purely D-puffed ones. So far, none of these three methods have led to a breakthrough in the  $q_{95}=3$  ITER BL scenario.

These three methods for ELM mitigation were also applied to the  $q_{95}=3.6$  scenario with similar results. In addition, phases with type-II ELMs were discovered in this scenario. In fig. 6 time traces of two  $q_{95}=3.6$  discharges are compared which mainly differ by the z-position of the plasma or by the closeness to a double-null configuration which is measured by the  $d_{\text{RXP}}$  parameter. The latter is the separation between the two flux surfaces which define the two X-points at the outer midplane. By reducing this parameter in the phase of full shaping from 1.5 to 1 cm (see fig. 6) after  $t=3\text{s}$ , type-I ELMs immediately disappear and a magnetic broad band signature appears typical for a type-II ELM scenario. Edge profiles do not significantly change, neither does energy and particle confinement. All empirical findings of these type-II ELMs are similar to previous type-II ELM studies at higher  $q_{95}$  [9] and to AUG results with a carbon wall [10].

Another step in  $d_{\text{RXP}}$  by 5mm after  $t=4\text{s}$  reduces the energy confinement by 15%. A nitrogen puff in the final phase of the discharge ( $5.6 < t < 6.2$ ) recovers energy confinement to an H-factor above 1. On AUG this well-known beneficial effect of nitrogen puffing on confinement at higher  $q_{95}$  and higher  $\beta_{\text{N}}$  [11] is here for the first time also clearly demonstrated for a  $q_{95}=3.6$  plasma with ITER-like shape, but has to be considered in this case as a non-stationary effect, since both tungsten concentration and radiation are strongly increasing shortly after the introduction of nitrogen. However, until now only rather moderate  $\text{D}_2$  and N gas puff levels were tried. The applied  $\text{D}_2$  and N levels might not lead to sufficient edge cooling, but might just increase W-sputtering. Therefore, the successful examples [4, 11] of other discharges at higher  $q_{95}$  and higher  $\beta_{\text{N}}$  having higher levels of  $\text{D}_2$  and N puffs will be tried during the next

campaign in this  $q_{95}=3.6$  scenario as well. In addition it will be tried to increase  $P_{ICRH}$  to counteract central impurity accumulation.

At first glance type-II ELMs seem to be a breakthrough for the development of a  $Q=10$  scenario with small ELMs. Unfortunately, type-II ELM scenarios in present day machines are known to exist probably only at high collisionality and might be therefore in view of ITER of less interest. However at present knowledge it is not clear whether the collisionality at the pedestal or close to the separatrix is the decisive parameter for the stability of type-II ELMs. In the latter case the prospect to establish a type-II ELM scenario in ITER becomes more realistic, since the collisionality close to the separatrix in ITER does not significantly differ from the one in present day tokamaks like AUG.

## 6. Helium Operation

In order to simulate the ITER operation in the non-nuclear phase, helium discharges have been performed at AUG. Since operation of the AUG NBI system with He was not possible at the time of the experiments, such He plasmas were heated with deuterium NBI and ECRH (1.1MA) or in the low  $I_p$  case (0.8MA) just with deuterium NBI. Thus, no 'pure' He operation on AUG was possible. Although pumping of He in AUG is rather ineffective, the operation of such He plasmas turned out to be unproblematic, once the appropriate (low) He puff level was found. Although the discharges were conducted more than 20 days after a boronization – a phase which was very challenging for operation of  $D_2$  ITER BL plasmas – no major operational difficulties were observed.

This is demonstrated in particular in fig. 7 where two discharges at 0.8MA / 1.4T are compared, one is  $D_2$  (red, #29977) fuelled the other one He fuelled (blue, 30011). At  $B_t=1.4T$  no central wave heating is available. Both discharges were conducted in a phase 20 days after a boronization. While  $D_2$  discharges typically start (still at low  $\delta$ ) to accumulate impurities (see tungsten concentration,  $c_w$ , upper, left box in fig. 7) under such wall conditions already at a time where the triangularity is still low, He discharges show a stationary behaviour with very low tungsten concentration  $c_w$  throughout the discharge. Around  $t = 2s$  both discharges have similar electron densities and temperatures. This is consistent with global stored energy  $W_{MHD}$  in  $D_2 \sim 1.5 W_{MHD}$  in He (see fig. 7).

In fig. 8 time traces for a He discharge at 1.1MA / 1.8T are shown. In particular  $f_{ELM}$  was between 200 and 300 Hz and the dependency with  $\delta$  is less pronounced compared to deuterium plasmas. High densities close to  $f_{GW}=1$  were reached. Even the switch-off of central

ECRH did not lead to W-accumulation.

The rising  $P_{\text{rad}}$  in fig. 8 is due to ECRF stray radiation (cut-off) disturbing the bolometer diagnostic rather than a sign of increasing core radiation. This interpretation is supported by the immediate reduction of  $P_{\text{rad}}$  once  $P_{\text{ECRH}}$  is zero and by the very low W concentration  $c_{\text{W}}$ , in particular in the phase with highest  $\delta$ .

Typically in such He discharges, electron densities are close to the Greenwald limit, energy confinement is low ( $H_{98y2} < 0.75$ ),  $f_{\text{ELM}}$  is high and triangularity does not have a significant impact on these parameters in contrast to the experience with deuterium plasmas. They even show stationary behaviour with unboronized walls and without centrally deposited wave heating which, in the case of deuterium discharges is mandatory.

In order to demonstrate that lessons learned in non-activating He operation can be transferred to later D or even D-T operation in ITER, AUG will put more effort into the development of target plasmas with lower He fuelling and hence obtain lower ELM frequency such that ELM mitigation with MP and pellet pacing can also be demonstrated in such He plasmas.

## 7. Summary and Conclusions

At AUG-W several  $q_{95}=3$  ITER BL demonstration discharges at  $I_p= 1.1$  and  $1.2\text{MA}$  were performed with ECRH and ICRH and showed stationary behaviour for many confinement times. Values for normalized density and energy confinement simultaneously came close to the requirements of the ITER BL scenario (see fig. 9) as long as  $\beta_N$  stayed above 2 (typically  $2.0 < \beta_N < 2.2$ ). At a lower heating power and thus at  $\beta_N = 1.8$  only H-factors around 0.85 have so far been achieved. Such low heated discharges were only stationary at  $D_2$  puffing rates around  $3 \cdot 10^{22} \text{ s}^{-1}$  and with a freshly boronized wall. The latter constraint is not a major problem for the extrapolation to ITER because the results of AUG-W with an intact, fresh boronization are the reference conditions for ITER with its Be/W wall. Boron-coated main chamber walls in AUG-W together with the tungsten divertor (typically not affected during a boronization process) simulate more closely the ITER situation of a Be main-chamber-wall and a tungsten divertor. The fact that in AUG-W no sufficient normalized confinement ( $H_{98y2} \sim 1$ ) has been found at low heating power ( $\beta_N = 1.8$ ) might be critical for ITER, since it suggests that significantly more additional heating would be required on this future device to achieve its goals. Previous results in AUG-C (see fig. 9) did not show this lack of confinement at low  $\beta_N$ . In AUG-C H-factors show only a much smaller decrease when heating power is reduced compared to the situation with metal walls in AUG-W. This different

behaviour between AUG-C and AUG-W is certainly also due to the operational necessity (for stationary conditions) in AUG-W to choose the gas puff rate sufficiently high in order to flatten steep tungsten density gradients in the H-mode edge transport barrier by frequent ELMs. However, for typical ITER parameters the neoclassical tungsten transport might even be outward drift dominated [12]. Therefore, the need to push ELM frequencies at ITER by high gas puff rates to tame the tungsten transport might be considerably reduced, which will without doubt have a beneficial effect on energy confinement.

As a possible alternative, the  $q_{95}=3.6$  scenario has been investigated. The operational window allowing stationary behaviour at the higher safety factor is definitely larger compared to the  $q_{95}=3$  scenario. Lower  $D_2$  puff rates are possible even under conditions of a diminishing boronization. Discharges with high normalized edge / pedestal density and at the target  $\beta_N$  value of 2.2 have been established (see fig. 10). In order to more closely match the line-averaged density of the  $q_{95}=3$  BL scenario, the peaking of the density profile has to be increased, which might be achieved by pellet fuelling. Normalized confinement in such discharges is above 1 but 12% below the target of  $H_{98y2} = 1.2$ . Thus also confinement has to be improved similar to the situation at  $q_{95}=3.0$ . This improvement might be achieved by N-seeding [11], which is a continuing topic of research. Also at JET with its ITER-like wall seeding of nitrogen in high- $\delta$  plasmas showed a beneficial effect on confinement [13, 14].

Very large ELMs, well above the established collisionality scaling [5], occurred in both scenarios, which appear difficult to mitigate. Three mitigation techniques (pellets, MP and N-seeding) have been tried, but did not show the desired effect. The solution for this problem remains the biggest challenge for optimizing such plasmas towards divertor heat load mitigation under steady-state conditions. As a side-result type-II ELM phases could be triggered by shifting the plasma closer to a double-null configuration. Seeding of nitrogen shows the first promising results in terms of improved confinement and reduced divertor temperature, but in both scenarios long-lasting stationary behaviour could not be reached until now.

The beneficial effect of higher triangularity to achieve simultaneously good confinement at high densities is similar in AUG-C and AUG-W (see left part of fig. 9) and thus confirms in this respect the choice for the ITER shape. However, higher triangularity is clearly also responsible for the occurrence of large low-frequent ELMs in these scenarios (see fig. 11) which are difficult to get rid of. Whether in total the ITER shape is a reasonable choice for an optimized ITER scenario cannot be answered at this stage. At least alternatives should be

considered in case the large ELMs occurring in high triangularity ITER demonstration plasmas cannot be suppressed or mitigated in present-day machines.

Finally for the operation in helium no major difficulties were observed. During a recent AUG campaign the operation of ITER BL scenario in He was successfully extended towards lower densities and higher ELM frequencies. Results on these experiments will be published elsewhere [15] in the near future and will help to answer the important question for ITER whether ELM control with MPs developed in  $D_2$  plasmas can be transferred to He plasmas and vice versa.

## 8. Acknowledgements

This work has been carried out within the framework of the EUROfusion Consortium and has received funding from the Euratom research and training programme 2014-2018 under grant agreement No 633053. The views and opinions expressed herein do not necessarily reflect those of the European Commission.

## 9. References

- [1] SIPS, A.C.C., et al., 24<sup>th</sup> IAEA Fusion Energy Conference 2012, San Diego [http://www-naweb.iaea.org/naweb/physics/FEC/FEC2012/papers/41\\_ITRP111.pdf](http://www-naweb.iaea.org/naweb/physics/FEC/FEC2012/papers/41_ITRP111.pdf)
- [2] SAIBENE, G. et al., Plasma Phys. Control. Fusion 44 (2002) 1769–1799
- [3] SCHWEINZER, J., et al., Europhysics Conference Abstracts 37D (2013), P2.134 <http://eps2013.aalto.fi/?page=proceedings>
- [4] BEURSKENS, M., Plasma Physics and Controlled Fusion 55 (2013), 124043 [doi:10.1088/0741-3335/55/12/124043](https://doi.org/10.1088/0741-3335/55/12/124043)
- [5] LOARTE, A. et al 2003 Plasma Physics and Controlled Fusion 45 1549
- [6] PEETERS, A., et al., Nucl. Fusion 47 (2007) 1341–1345
- [7] LANG, P.T. et al., Nucl. Fusion 54 (2014), 083009
- [8] SUTTROP, W., et al., Phys. Rev. Lett. 106, 22 (2011), 225004
- [9] WOLFRUM, E. et al., Plasma Physics and Controlled Fusion 53, 8 (2011), 085026
- [10] STOBER, J. et al., Nucl. Fusion 41 (2001), 1123-1134
- [11] SCHWEINZER, J., et al., Nucl. Fusion 51 (2011) 113003 [doi:10.1088/0029-5515/51/11/113003](https://doi.org/10.1088/0029-5515/51/11/113003)
- [12] DUX, R., et al., *Europhysics Conference Abstracts (CD-ROM, Proc. of the 40th EPS Conference on Plasma Physics, Espoo, Finland, 2013)*, (Ed.) V. Naulin and C. Angioni and M. Borghesi and S. Ratynskaia and S. Poedts and T. Donné and T. Kurki-Suonio and S. Äkäslompolo and A. Hakola and M. Airila (European Physical Society, Geneva), Vol. 37D (2013), P4.143
- [13] GIROUD, C. et al., Nucl. Fusion 53 (2013) 113025 [doi:10.1088/0029-5515/53/11/113025](https://doi.org/10.1088/0029-5515/53/11/113025)
- [14] GIROUD, C. et al., Plasma Phys. Control. Fusion 57 (2015) 035004 [doi:10.1088/0741-3335/57/3/035004](https://doi.org/10.1088/0741-3335/57/3/035004)
- [15] PÜTTERICH, T., private communication

**Figures & Captions:**

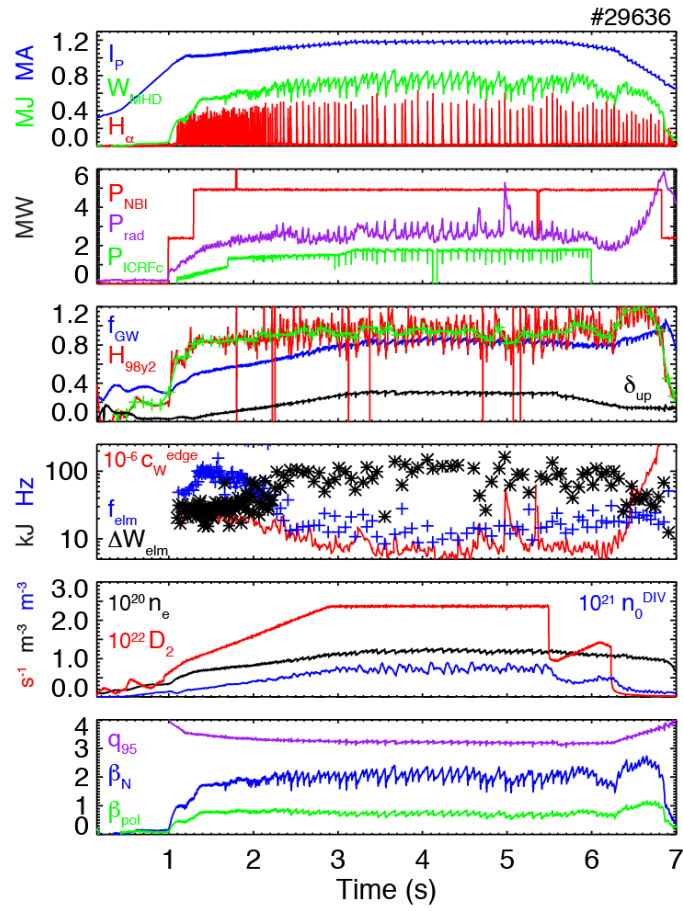


FIG. 1.: Time traces of 1.2MA / 2T ITER BL discharge (#29636) centrally heated by ICRH.

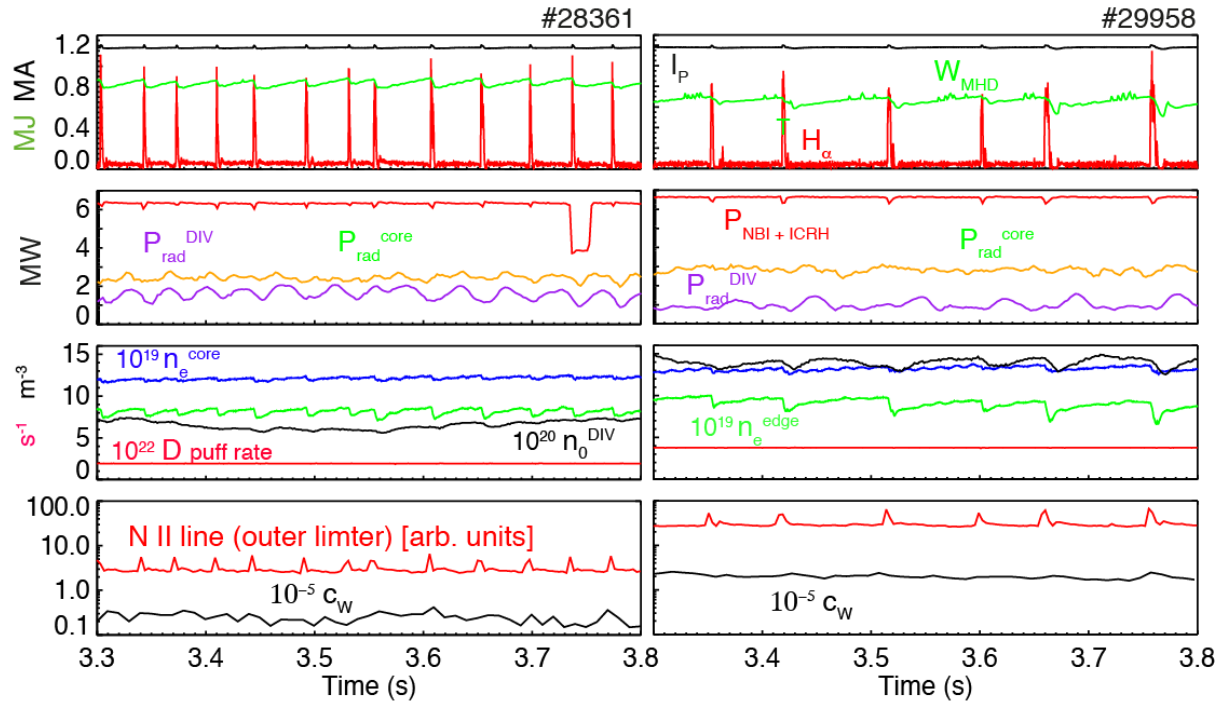


FIG. 2.: Comparison of ITER BL discharges during phases of 0.5s. Discharge parameters are identical except gas puff and ‘freshness’ of boronization. While the discharge on the left (#28361) was conducted 1 day after a boronization, the one on the right (#29958) was done 21 days after a boronization. Different gas puff levels  $1.9 \cdot 10^{22}$  and  $3.8 \cdot 10^{22}$  were necessary to reach stationarity for discharges #28361 and #29958, respectively.

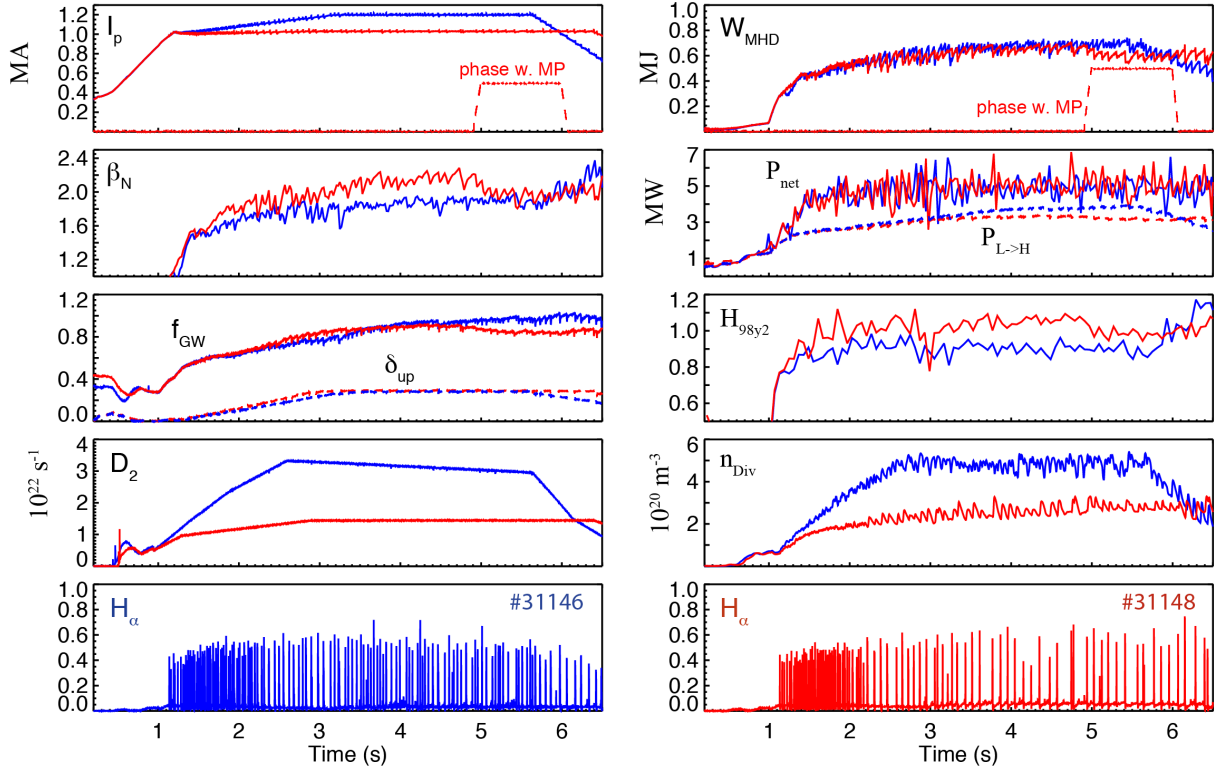


FIG. 3.: Time traces of various parameters (plasma current  $I_p$ , stored energy  $W_{MHD}$ , normalized pressure  $\beta_N$ , net heating power  $P_{net}$ , H-mode power threshold  $P_{L \rightarrow H}$ , Greenwald fraction  $f_{GW}$ , upper triangularity  $\delta_{up}$ , H-mode factor  $H_{98y2}$ ,  $D_2$  puff rate, neutral gas density in the divertor  $n_{Div}$ , ELM signature  $H_\alpha$ ) for a comparison of a  $q_{95}=3$  (#31146, blue) with a  $q_{95}=3.6$  (#31148, red) discharge. For both discharges the toroidal field  $B_t = 2T$ , the applied heating power (NBI + ICRH) as well as the plasma shape are the same.



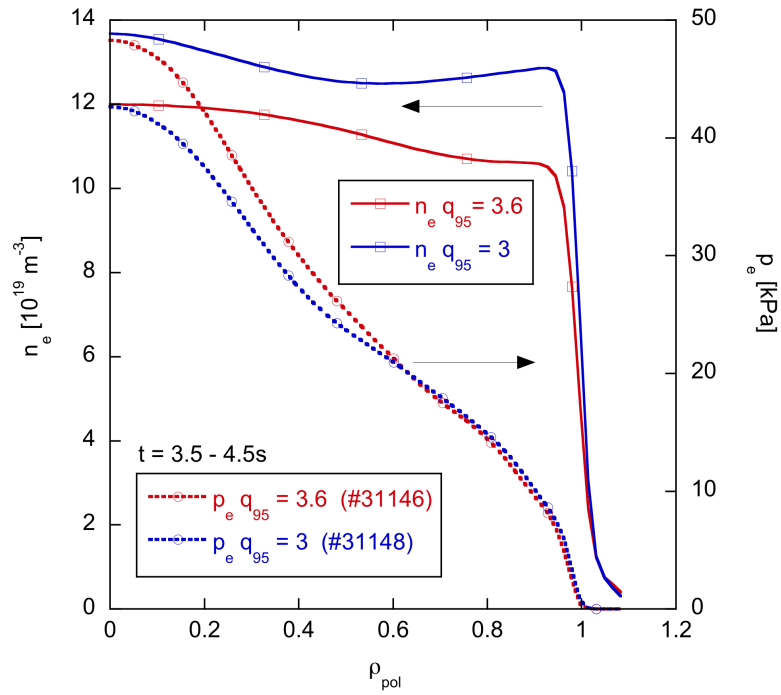


FIG. 4.: Radial profiles of electron density  $n_e$  and electron pressure  $p_e$  for the discharges of fig. 2 at  $q_{95}=3$  (#31148, blue) and  $q_{95}=3.6$  (#31146, red) averaged from 3.5s to 4.5s.

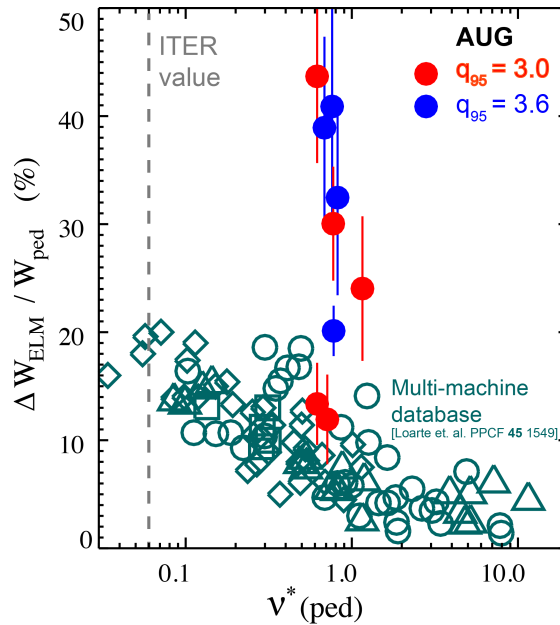


FIG. 5.: Energy loss of Type-I ELMs normalized to the pedestal stored energy vs. collisionality of the pedestal (value for ITER indicated by broken vertical line). Values for the two AUG scenarios at  $q_{95}=3.0$  and  $q_{95}=3.6$  are compared to a multi-machine scaling [6].

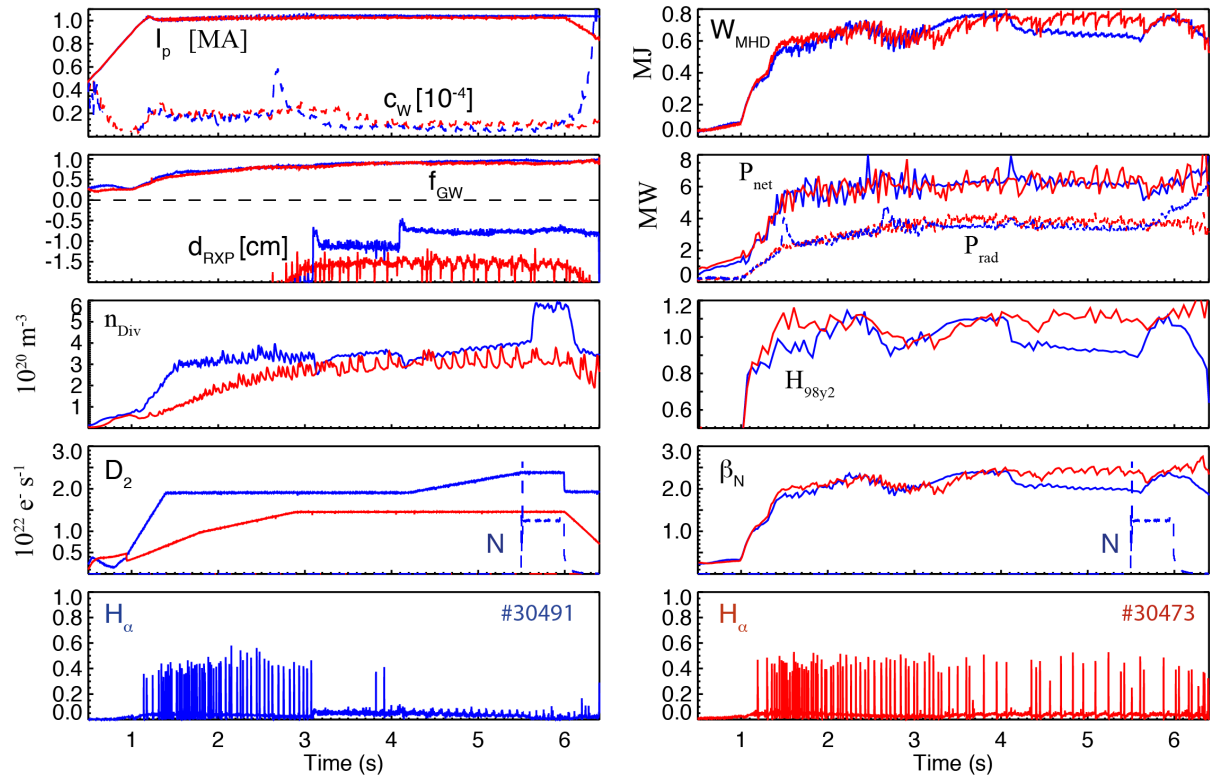


FIG. 6.: Time traces of various parameters (radiated power  $P_{rad}$ , separation of X-points  $d_{RXP}$ , nitrogen puff rate  $N$ ) for two  $q_{95}=3.6$  discharges (#30491 with a type-II ELM phase, blue;) with different closeness ( $d_{RXP}$ ) to double-null configuration. For both discharges the toroidal field  $B_t = 2T$ , the applied heating power (NBI + ICRH) as well as the triangularity are the same.

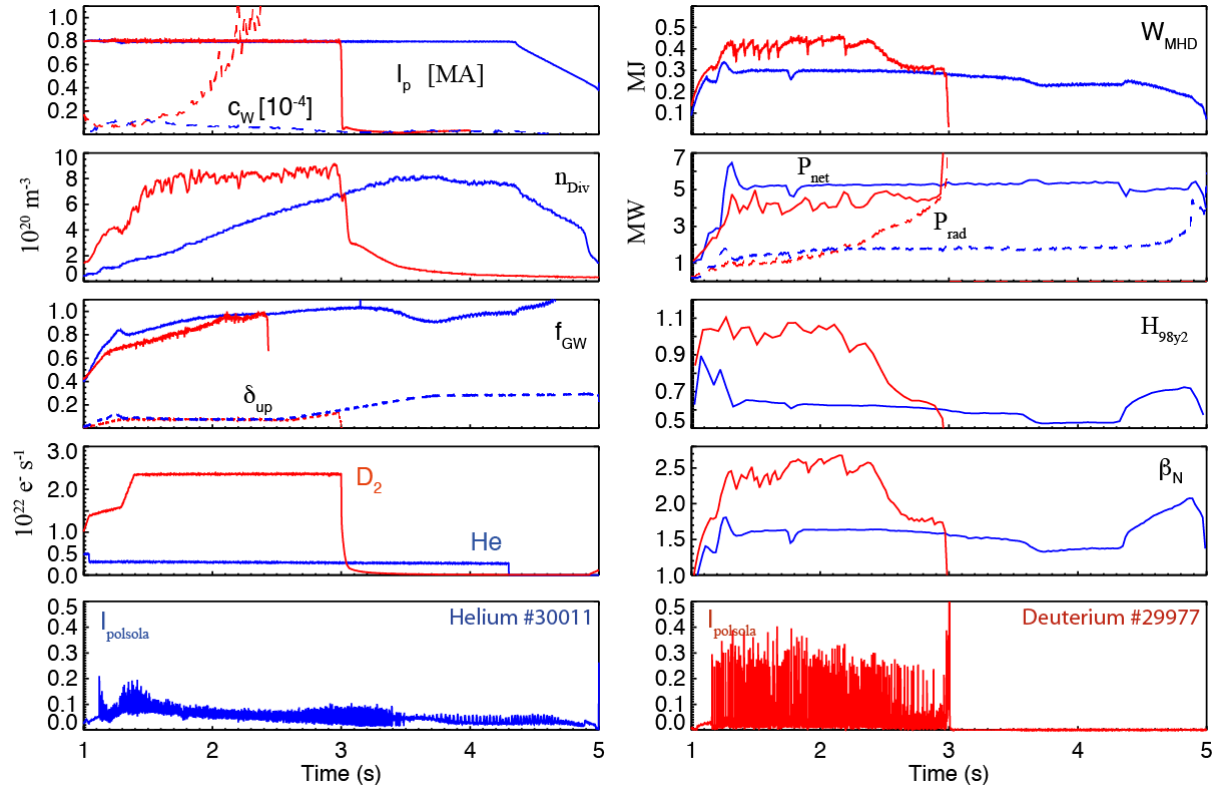


FIG. 7.: Time traces of various parameters ( $D_2$  / He puff rate, ELM signature  $I_{polsola}$ ) for a comparison of a  $q_{95}=3$  He discharge (#30011, blue) with a  $q_{95}=3$   $D_2$  (#29977, red) discharge.

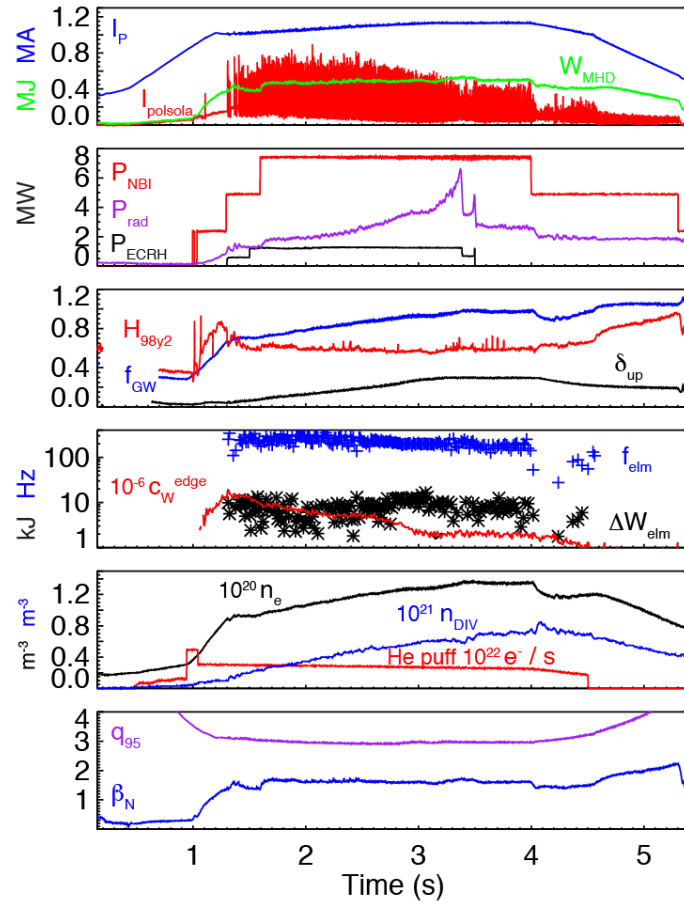


FIG. 8.: Time traces, of an ECRF-heated He discharge #30015 (1.1MA / 1.8T, further details, see text)

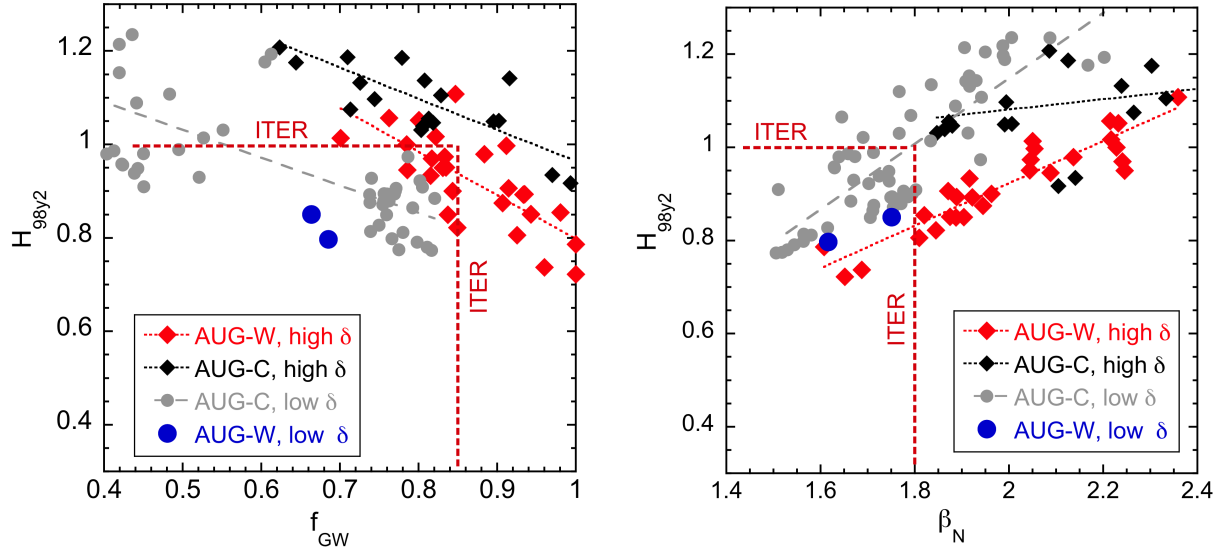


FIG. 9.: Normalized confinement  $H_{98y2}$  vs. density  $f_{GW}$  (left) and pressure  $\beta_N$  (right) for operation at  $q_{95} = 3$ . Target values for the ITER BL scenario are indicated by red lines.

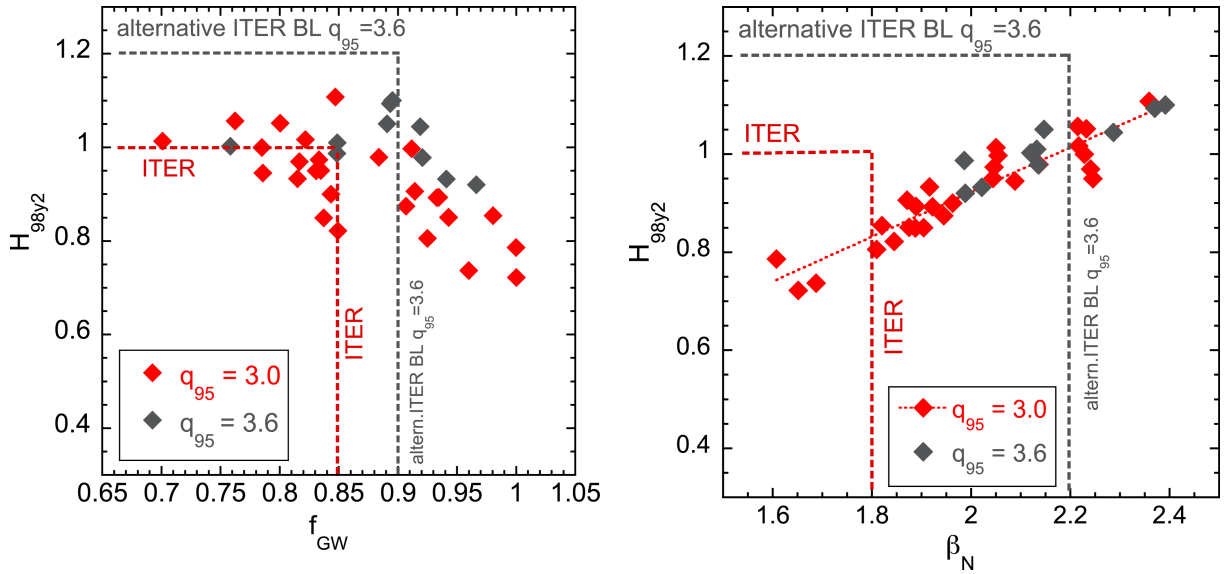


FIG. 10.: Normalized confinement  $H_{98y2}$  vs. density  $f_{GW}$  (left) and pressure  $\beta_N$  (right) for operation at  $q_{95} = 3$  (red) and  $q_{95} = 3.6$  (green) in AUG-W (high  $\delta$ ). Target values for the ITER BL scenario and the alternative ITER BL scenario are indicated by red and green broken lines, respectively.

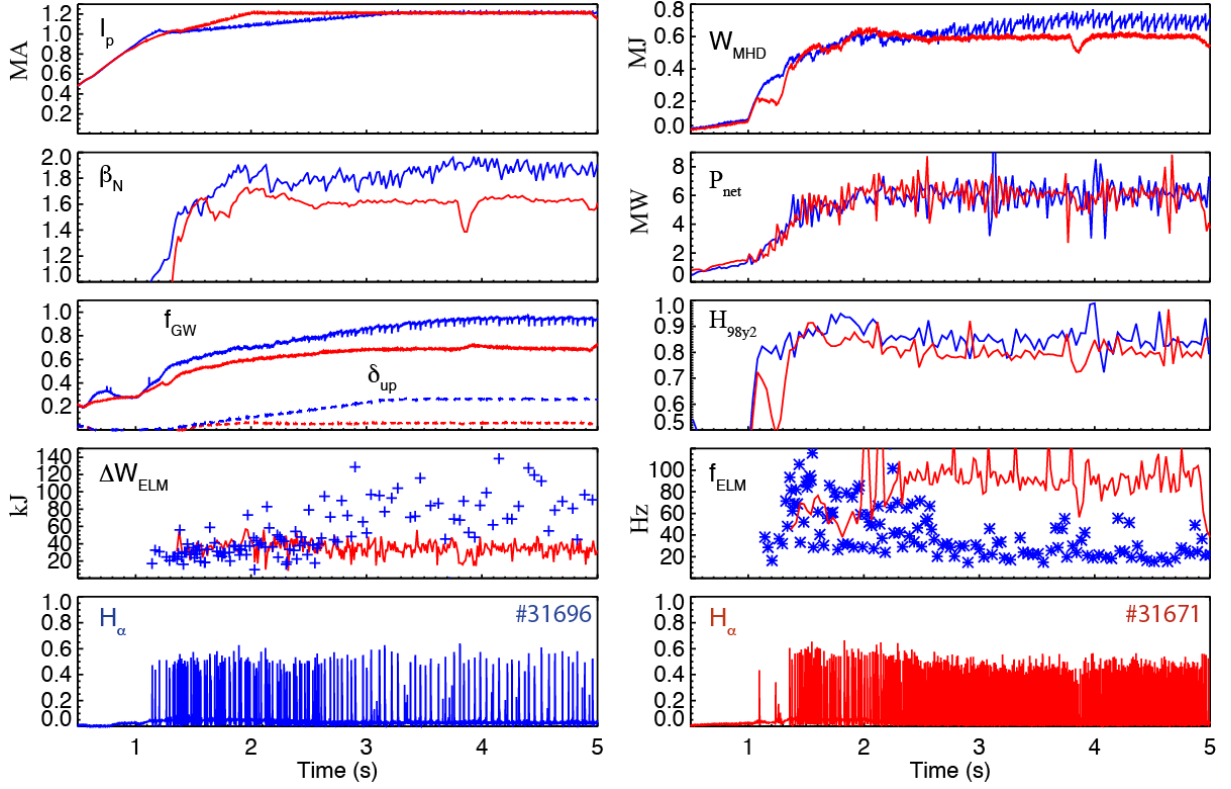


FIG. 11.: Time traces of various parameters (plasma current  $I_p$ , stored energy  $W_{MHD}$ , normalized pressure  $\beta_N$ , net heating power  $P_{net}$ , Greenwald fraction  $f_{GW}$ , upper triangularity  $\delta_{up}$ , H-mode factor  $H_{98y2}$ , energy loss per ELM  $\Delta W_{ELM}$ , ELM frequency  $f_{ELM}$ , ELM signature  $H_\alpha$ ) for a comparison of a  $q_5 = 3.1$  (#31671, blue) discharge at high triangularity ( $t > 3s$ ) with a  $q_5=2.9$  (#31694, red) discharge at low triangularity. For both discharges the toroidal field  $B_t = 2T$ , the applied heating power (NBI + ICRH) as well as the high gas puff rate of  $6 \cdot 10^{22} s^{-1}$  are the same.